

Biophysical Journal, Volume 114

Supplemental Information

**Single-Molecule Assay for Proteolytic Susceptibility: Force-Induced
Collagen Destabilization**

Michael W.H. Kirkness and Nancy R. Forde

Supporting Note 1: Mini-Radio Centrifuge Force Microscope (MR.CFM)

Design and Use

Centrifuge

MR.CFM fits within a single bucket of a Beckman Coulter Allegra X-12R centrifuge, equipped with an SX4750A ARIES "Swinging Bucket" Rotor Assembly. The centrifuge is refrigerated, enabling easy access to temperature-controlled single-molecule force assays. Design constraints from this bucket assembly are its rotational arm length of 207.8 mm, a maximal rotational speed of 3750 RPM, and a maximum fluid mass per bucket of 750 g, with an imbalance tolerance of ± 50 g.

MR.CFM Microscope

The use of a benchtop centrifuge prescribed three design limitations: overall height (180 mm) and mass (750 g) (set by the specific centrifuge and rotor), and the need for wireless communication and power. The final microscope accommodates all of these constraints, with a height of 154 mm, a mass of 421 g (including batteries), and fully wireless operation. MR.CFM is depicted in Figure 2 of the main manuscript. The instrument was built using as many commercial parts as possible for ease of reproduction. Schematics and parts lists are provided in Supporting Figure 1 and Supporting Table 1. Note that, while the designs provided are specific to this rotor assembly, MR.CFM can easily be adapted for other benchtop centrifuges, primarily by modifying the base.

MR.CFM is composed of two parts, the optical assembly and the base, which provides support and acts as a sample holder. A hard, closed-cell plastic (Sintra) formed the bulk of the base, chosen for its high rigidity and low mass. An aluminum insert was included directly below the microscope within this base to strengthen the rigidity of the assembly under high load and provide support for the sample chamber. These parts were machined to fit snugly into the centrifuge bucket (Supporting Figure 2 and Supporting CAD drawings).

The optical path comprises an LED light source, ground glass diffuser, sample chamber, infinity-corrected objective lens, tube lens, and CCD camera with lens (Supporting Figure 1c and Supporting Table 1). The LED light source and ground glass diffuser are housed within the aluminum insert while the sample chamber slides into the sample holder on top of the aluminum insert (Supporting Figure 2). The LED and sample chamber are held in place simply by friction, which facilitates their replacement, while the diffuser is glued (JB Weld Original) into the insert. The remaining components in the optical path are mounted within stacking lens tubes. The following non-standard-sized parts are glued into place using epoxy (JB Weld Original): aluminum base insert, inner portion of the objective lens CCD camera with lens and extension mount (see below). The tube lens is held in place using a counter-threaded locking ring. The microscope's focal distance is modified by manually rotating two adjustable lens tubes, thereby altering the distance between the objective and tube lens. The focus is locked in place by tightening a counter-threaded locking ring. Two parts were removed from the objective lens: a rubber spacer from the lens stack (which resulted in a significantly enhanced stability of the working distance under force) and the outer casing (which reduced the mass by 67 g).

Pixel size in the microscope field of view was determined to be 0.43 $\mu\text{m}/\text{px}$, using a transmission electron microscopy grid (Ted Pella) and analysis using ImageJ.

Supporting Note 2: Image Acquisition and Analysis

The image analysis workflow acquires, processes and analyzes data from the raw images acquired by MR.CFM (Figure 3). The camera produces a wireless analog signal, which is received by the radio AV receiver. The transfer rate is 28 frames per second. In this step, there is some inherent interference that is coupled to the rotation frequency of the rotor with MR.CFM. Experimentally, this interference can be minimized by placing the AV receiver directly above the rotor's spindle. A USB analog-to-digital converter converts the analog signal from the AV receiver to digital. The signal is then acquired by a computer program, Totalmedia 3.5 (ArcSoft), which permits storage and viewing of the image stream in real-time. Real-time transfer of the data to an external computer is beneficial as it allows for essentially unlimited storage, permitting extremely long run times. In our instrument, run lengths are hardware-limited by battery lifetimes: three hours of continuous measurement are possible with two 9 V batteries wired in parallel to power the camera; this is easily increased by the addition of more batteries in parallel.

Efficient analysis requires the ability to count hundreds to thousands of particles reliably. The image processing used in this work minimizes user input and is implemented within a semi-automated ImageJ macro (code provided online). First, to remove any interference remaining in the signal (arising from rotation of the microscope about the receiver), a 10-image median z-stack algorithm is first applied, which eliminates the interference. Next, a rolling ball subtraction method (50 pixels) is applied, which improves image quality by subtracting the image background. The script then inverts the images and sums five images to increase contrast. Before counting, we mask regions corresponding to uncountable regions (such as multiple particle

clusters and dust). In cases where the contrast is not sufficient, a local adaptive thresholding plugin is used prior to particle counting, which removes the background completely.

Supporting Note 3: Proteolysis of Collagen and DNA by Trypsin

Surface Chemistry

For highly multiplexed experiments in the MR.CFM, it is essential to have a high surface coverage of beads, each bound to the surface by a single collagen molecule. Here, we implemented a blocking and specific tethering system that relies on a self-assembled monolayer (SAM) of Tween-20 for blocking and on biotinylated BSA for specific tethering.¹ To form the SAM, glass slides and coverslips were cleaned and activated through a series of washes with potassium hydroxide and organic solvents, followed by a coating of dichlorodimethylsilane (DDS). DDS (Sigma 440272) creates a strongly hydrophobic surface on the glass slide. Self-assembly of the Tween-20 surfactant resulted in a densely coated short PEG layer to block nonspecific binding of both the microspheres and enzymes (Figure 2d). To enable specific binding, biotinylated BSA was applied before Tween-20, and was bound by streptavidin.

The detailed protocol followed Hua *et al.*,¹ with the following minor modifications. As stated above, glass coverslips and slides were used, and a glass dish was used for coating rather than a glass slide holder. Thus, we used 200 ml of hexane and 133 μ l DDS. Assembly of our chambers used JB Weld instead of double-sided tape. For the surface coating, we incubated for 10 minutes with 0.5 mg/ml biotinylated BSA (Sigma A8549) in 20 mM Tris and 50 mM NaCl, pH 8.0; followed by 10 minutes with 0.2% Tween-20 (Sigma P9416); followed by a 5-minute incubation with 0.5 mg/ml streptavidin (Sigma S4762) in 20 mM Tris and 50 mM NaCl, pH 8.0. Final washing steps were performed using our reaction buffer of 100 mM Tris, 400mM NaCl, pH 7.4.

Collagen Functionalization and Tethering

Recombinant human type III collagen (Fibrogen FG-5016) was end-labelled for manipulation as described.² Briefly, its N-terminus was labeled with a biotin via aldehyde functionalization (PLP, Sigma P9255) and further reaction with biotin hydrazide (Sigma B7639) to form a covalent hydrazone bond with the introduced aldehyde. The success of the reaction was confirmed with Western blots using streptavidin alkaline phosphatase. Biotinylated collagen was tethered to the bead via its unique C-terminal cysteine residues. Amine-functionalized superparamagnetic microspheres (M270 Dynabeads) were modified by reaction with an SPDP linker (Pierce 21857). Concurrently, collagen was reduced with TCEP reducing gel (Thermo Scientific 77712) to present thiols. Incubation of reduced collagen with SDPD-functionalized beads allowed for the formation of disulfide bonds between beads and collagen proteins. The ratio of collagen:beads for this reaction was adjusted to achieve single-molecule tethers, as follows.

As the ratio of collagen:beads was decreased in this final coupling step, we observed that the number of beads bound to the surface decreased. This implied that collagen concentration was the limiting factor for forming tethers, suggesting we were in the single-tether range. To confirm that single tethers were linking the beads to the surface, we visually inspected the beads at high magnification to confirm constrained, two-dimensional Brownian motion.

DNA Preparation

To use the same surface conjugation methods as for collagen, DNA end-labelled with thiol and aldehyde reactive groups was produced via PCR from the pUC19 plasmid. The PCR product was 969 bp, approximately the same contour length as collagen (~300 nm). The PCR used a thiol-

modified primer, 5'-Thiol TTG CTT GAT ATC TTG TAC TGA GAG TGC ACC-3', and an aldehyde-modified primer, 5'- Aldehyde TGT CTT AGA TCT TTT GGA GCG AAC GAC-3' (both from Bio-Synthesis). DNA was tethered to the amine-functionalized microspheres (M270 Dynabeads) via the same reaction pathway as collagen.

Single-Molecule Proteolysis Experiments

Immediately prior to measurements, trypsin and labelled (DNA or collagen) beads were mixed and injected into the sample chamber. The sample chamber was sealed with melted paraffin wax and placed upside down for approximately five minutes to allow the labelled beads to settle and bind to the desired surface. The chamber was then inverted and inserted into MR.CFM, its focus was adjusted, and the entire MR.CFM was placed in the centrifuge. When the centrifuge reached the desired rotation rate (for these experiments, 800 rpm), image recording (Totalmedia 3.5) was initiated on the remote computer. Parallel experiments with collagen (or DNA) under ~zero force (67 fN, the force of gravity on the beads) were conducted essentially as above, but with imaging performed using a bright-field microscope (Olympus BX51, equipped with 10X Plan N objective) and CCD camera (Flea, Point Grey Research), and with images acquired using National Instruments LabVIEW.

The force acting on the beads in MR.CFM was calculated from $F=m\omega^2r$, where the rotational arm length $r=18.2$ cm from the centre of the spindle to the sample chamber, and the mass of the beads relative to water $m=6.9\times 10^{-12}$ g is obtained from the manufacturer-specified bead density (1.6 g/cm³) and size (2.8 μ m diameter), which has been validated previously in single-molecule force measurements.³

Experimental Replicates and Error Determination

Multiple replicates were performed as follows. Trypsin force experiments include data from six separate runs, on four different days, with a total number of initial particles of $N=4903$. Trypsin zero-force experiments include data from four separate runs, on four different days, with $N=12131$. No enzyme, force experiments use data from three separate runs, on three different days, with $N=1493$. No enzyme, zero-force experiments use data from two separate runs, on two different days, with $N=4252$. Complete data sets are shown in Supporting Figure 5.

Supporting Table 1 – MR.CFM parts list

<u>Component</u>	<u>Description, source, part number and price (USD)</u>
Base	Sintra plastic, machined as in Supporting Figure 2. Approximate cost for starting material: \$20 (Associated Plastics).
Base insert	Aluminum, machined as in Supporting Figure 2. Approximate cost for starting material: \$3 (Metal Supermarkets).
LED with holder	5W white. Super Bright LEDs Inc. VL-H01xWx5 (\$7)
Ground Glass Diffuser	Thor Labs DG05-120 (\$13)
Infinity-corrected objective lens	40X, NA 0.65, air. Nikon (<\$500)
Lens tubes with internal and external locking rings	2x Stackable; 1” diameter. ThorLabs SM1L10 (\$15) 3x Adjustable; 1” diameter. ThorLabs SM1V10 (\$35)
Tube lens	40 mm focal length. Thor Labs LA1422 (\$22)
Camera lens	Included with camera.
Camera lens extension mount	Aluminum, machined to provide desired magnification (Supporting Figure 2). Approximate cost for starting material: \$1 (Metal Supermarkets).
Wireless CCD Camera	Security Color Mini Spy Pinhole CCD Wireless Camera. RC Hobbies Outlet 73724810. Alternatively, HDE Pinhole Mini Wireless Camera, Amazon (\$25)
Lithium 3V “coin” batteries	2x2032; widely available (\$1)
9V Batteries + snap connector clips	Widely available (\$1)
Radio AV Receiver	Included with wireless camera
TV Tuner	AVI TV Wonder HD 750 USB. Alternatively, StarTech S-Video / Composite to USB Video Capture Cable, B&H (\$35)

Supporting Table 2 – Rate constants from combined replicates

Experiment	k_{eff} (min^{-1})	k_{ns} (min^{-1})	k_{Tr} (min^{-1})
-trypsin, $F=0$	--	0.010 ± 0.013	--
+trypsin, $F=0$	0.018 ± 0.001	$0.010^* \pm 0.013$	0.007 ± 0.013
-trypsin, $F=9$ pN	--	0.137 ± 0.005	--
+trypsin, $F=9$ pN	0.364 ± 0.037	$0.137^* \pm 0.005$	0.227 ± 0.037

Rate constants were determined by weighting $f(t)$ determined from the total number of beads remaining at each time ($f(t) = N_{\text{tot}}(t)/N_{\text{tot}}(0)$) by the counting error ($1/\sqrt{N}$).

*Values from the no-enzyme fits were used to determine the trypsin-dependent rate constants, using equations (1) and (2).

Supporting Table 3 – Rate constants from individual collagen replicates

Experiment	Replicate number	Initial number of beads	k_{eff} (min^{-1})	$\langle k_{\text{eff}} \rangle$ (min^{-1})	$\langle k_{\text{ns}} \rangle$ (min^{-1})	$\langle k_{\text{Tr}} \rangle$ (min^{-1})
-trypsin, $F=0$	1	1929	0.009 ± 0.015	--	0.011 ± 0.002	--
	2	2323	0.012 ± 0.019			
+trypsin, $F=0$	1	3461	0.050 ± 0.008	0.039 ± 0.020	$0.011^* \pm 0.002$	0.028 ± 0.021
	2	2918	0.054 ± 0.010			
	3	3384	0.009 ± 0.001			
	4	2368	0.044 ± 0.006			
-trypsin, $F=9$ pN	1	775	0.163 ± 0.010	--	0.160 ± 0.003	--
	2	182	0.157 ± 0.022			
	3	536	0.160 ± 0.020			
+trypsin, $F=9$ pN	1	935	0.210 ± 0.008	0.362 ± 0.188	$0.160^* \pm 0.003$	0.202 ± 0.188
	2	860	0.360 ± 0.011			
	3	501	0.188 ± 0.010			
	4	743	0.281 ± 0.010			
	5	1187	0.436 ± 0.006			
	6	677	0.697 ± 0.032			

Errors on the individual k_{eff} represent 1σ on the fit parameters. The error on each mean rate constant represents the standard deviation of the individual k_{eff} values.

Replicates with force were fit to 20 minutes. Replicates without force were fit to 60 minutes, with the exception of replicate 3 with trypsin, which was fit to 180 minutes to permit fit convergence.

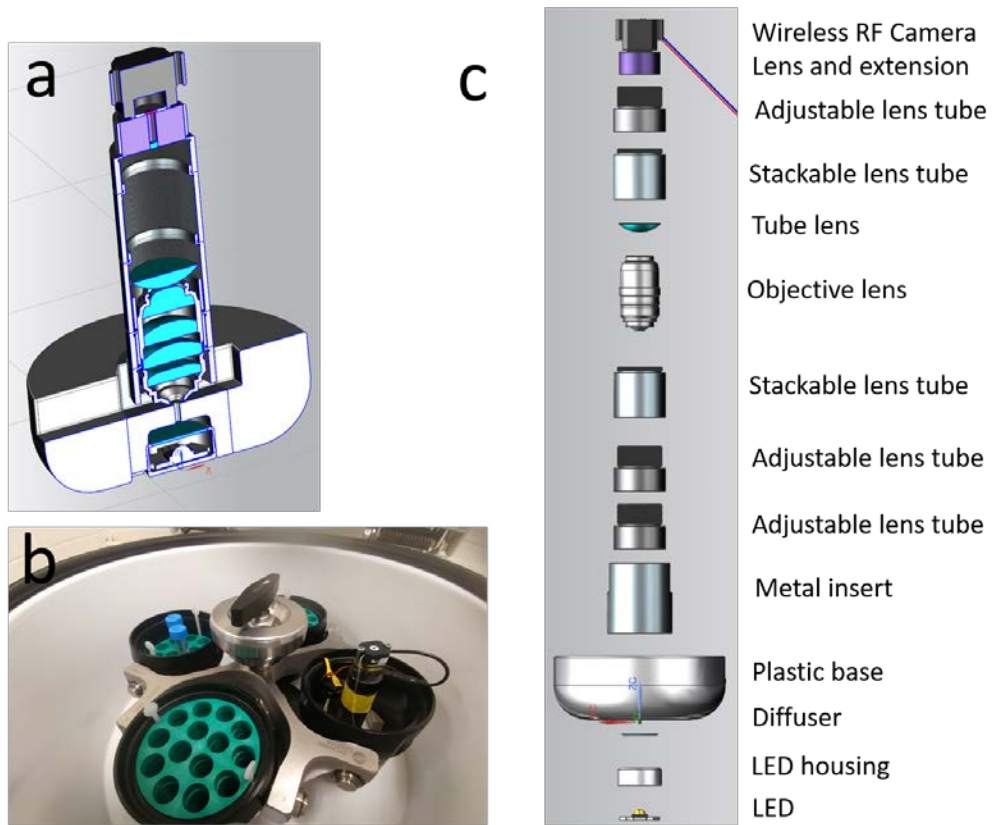
*Values from the no-enzyme fits were used to determine the trypsin-dependent rate constants, using equations (1) and (2).

Supporting Table 4 – Rate constants from individual DNA replicates

Experiment	Replicate number	Initial number of beads	k_{eff} (min^{-1})	$\langle k_{\text{eff}} \rangle$ (min^{-1})	$\langle k_{\text{ns}} \rangle$ (min^{-1})	$\langle k_{\text{Tr}} \rangle$ (min^{-1})
-trypsin, $F=0$	1	622	0.006 ± 163	--	0.026 ± 0.012	--
	2	833	0.041 ± 0.27			
+trypsin, $F=0$	1	250	0.205 ± 0.277	0.140 ± 0.092	$0.026^* \pm 0.012$	0.114 ± 0.092
	2	1029	0.124 ± 0.049			
-trypsin, $F=9$ pN	1	18	0.138 ± 0.055	--	0.233 ± 0.032	--
	2	168	0.270 ± 0.018			
	3	83	0.256 ± 0.015			
	4	252	0.248 ± 0.039			
	5	369	0.206 ± 0.028			
+trypsin, $F=9$ pN	1	150	0.120 ± 0.015	0.217 ± 0.08	$0.233^* \pm 0.032$	~0
	2	41	0.180 ± 0.035			
	3	242	0.200 ± 0.008			
	4	220	0.232 ± 0.010			
	5	113	0.366 ± 0.023			

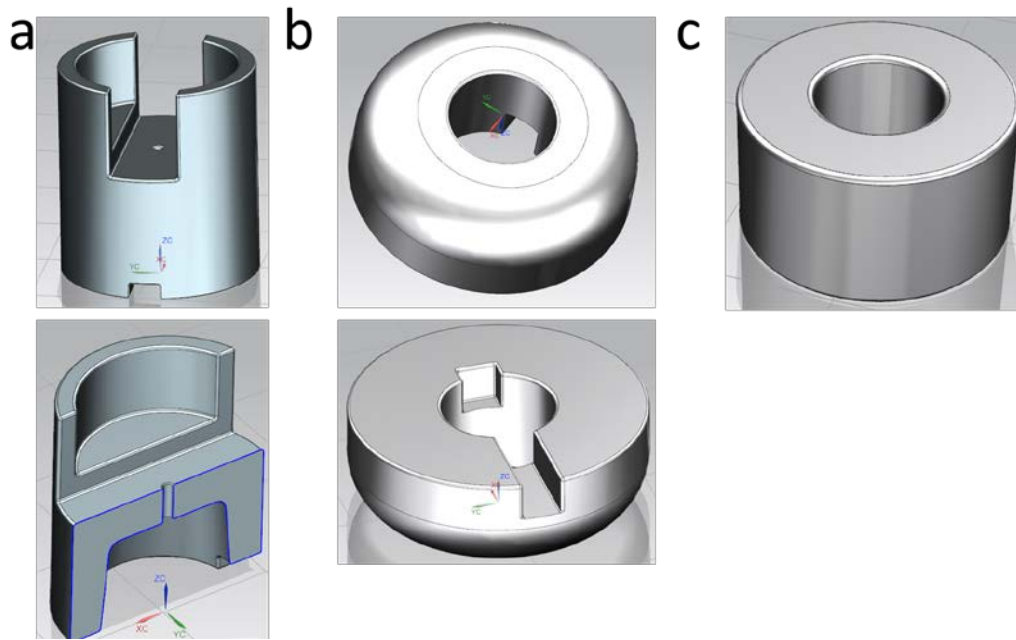
Errors on the individual k_{eff} represent 1σ on the fit parameters. The error on each mean rate constant represents the standard deviation of the individual k_{eff} values.

*Values from the no-enzyme fits were used to determine the trypsin-dependent rate constants, using equations (1) and (2).

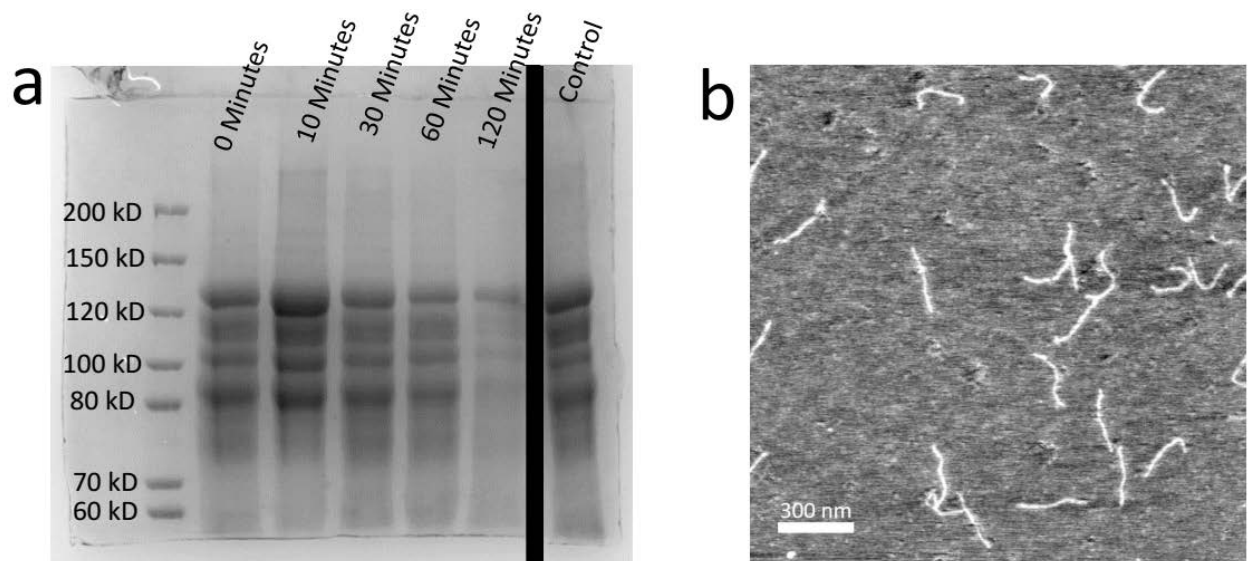


Supporting Figure 1. MR.CFM model and assembly. a) To-scale 3D rendering of MR.CFM.

MR.CFM fits inside a centrifuge bucket and has a total height of 154 mm and mass 421 g, including batteries. b) MR.CFM is shown inside a centrifuge bucket within a Beckman Coulter Allegra X-12R centrifuge (SX4750A ARIES™ Rotor Swinging Bucket). c) Assembly of parts of MR.CFM.

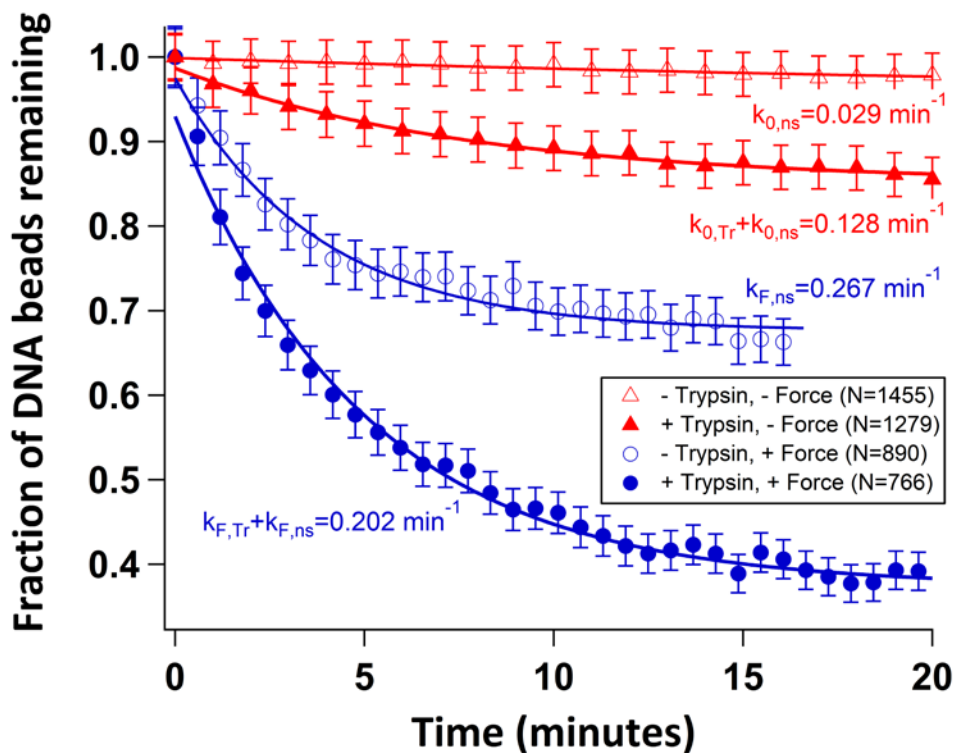


Supporting Figure 2. Drawings of the custom-made parts. (a) Sintra plastic base. (b) Aluminum base insert with sample chamber slot. (c) Pinhole lens extension mount. CAD drawings are available as Supporting Files online.

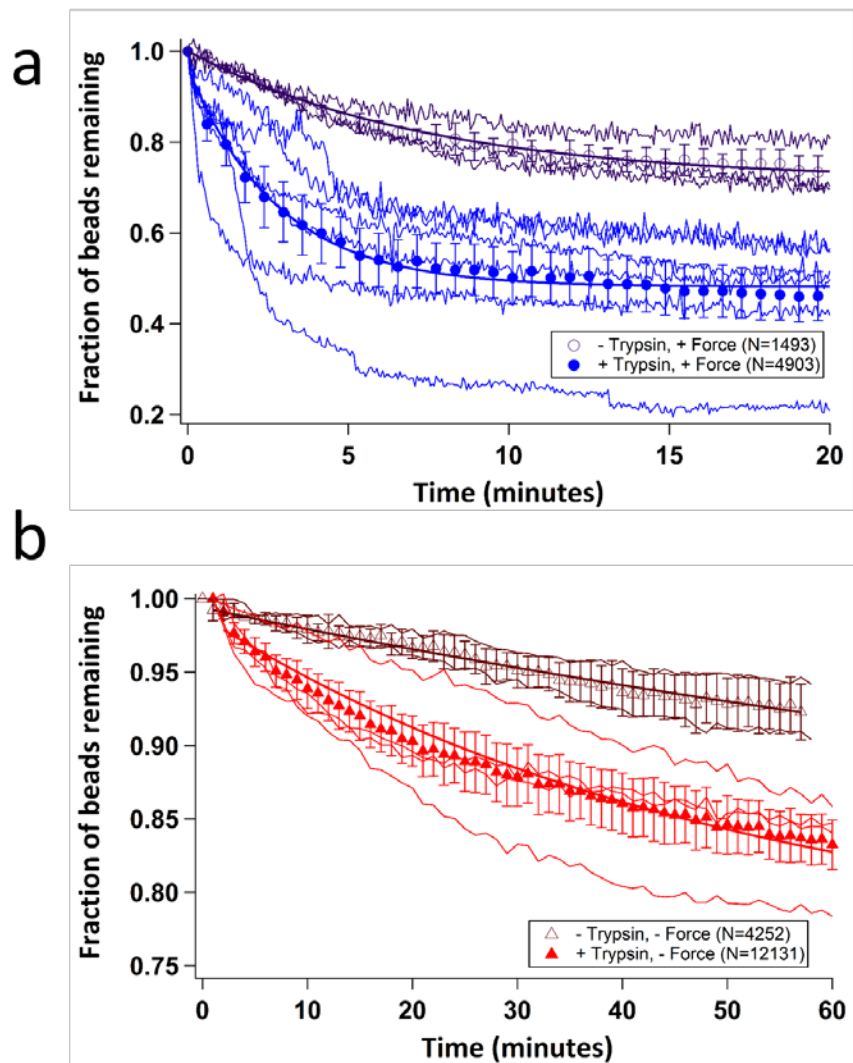


Supporting Figure 3. Time-dependent trypsin cleavage of type III collagen and AFM

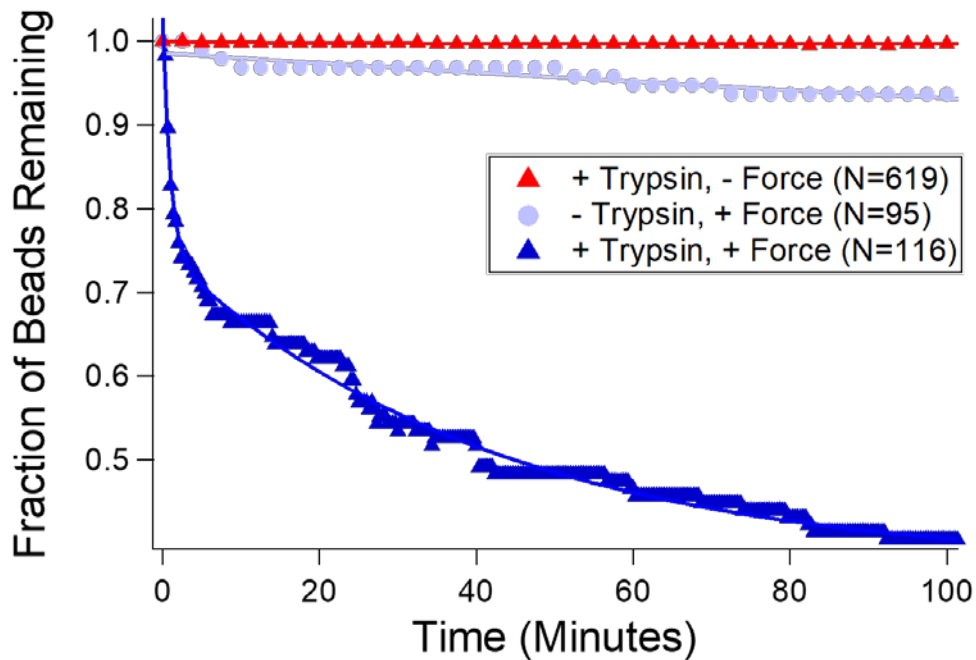
characterization. (a) Trypsin can cleave collagen at room temperature without force, as noted by the gradual disappearance of defined bands in the gel. The conditions for the reaction are 2 mg/ml type III collagen and 1 μ g/ml trypsin (a much lower concentration than used in the single-molecule assays), in a buffer of 0.1M Tris, 0.4M NaCl at a pH of 7.4. Aliquots were removed at 0, 10, 30, 60 and 120 minutes respectively, then heated for 10 minutes at 90°C in the presence of β -mercaptoethanol. The samples were run on a 6% SDS-PAGE gel and stained with a solution of Coomassie blue. Of note, SDS-PAGE gels of pure collagen can exhibit shorter bands (as seen here, running at approximately 115, 100, and 80 kDa), which likely arise from acid-induced hydrolysis at 90°C.⁴ The stock solution is monodisperse, as seen in (b), AFM image of type III collagen molecules. Analysis of contour lengths from this and other images gives 269 \pm 2 nm ($N=33$), demonstrating that the collagen sample is monodisperse. Collagen was deposited from 1 mM HCl, 100 mM KCl onto mica and then dried prior to imaging. Images were recorded with an Asylum Research MFP-3D SPM in tapping mode, with Mikromasch HQ:NSC15/AL BS tips.



Supporting Figure 4. DNA molecules tethered using the same linking chemistry do not exhibit a force-enhanced cleavage rate by trypsin. This demonstrates that the streptavidin and BSA linking proteins are not responsible for the force-induced susceptibility to proteolysis. Here, the data from all replicates are pooled to provide the overall fraction of beads remaining as a function of time. Error bars represent $\sqrt{N(t)}$ counting errors. The fraction of beads remaining as a function of time is well described by a single exponential decay. The effective rate constants resulting from fitting these data are shown in the figure. Rate constants from single exponential fits to each replicate are reported in Supporting Table 4 and do not differ significantly from the values shown here. Both approaches find that the trypsin-dependent cleavage rate k_{Tr} is not enhanced by force.



Supporting Figure 5. Full data sets for single-molecule collagen experiments, shown separately as (a) with force and (b) without force. Individual replicates are shown as thin lines (with variation due to imperfect counting of very large numbers of beads), and the average fraction remaining is shown in symbols, corresponding to Figure 4a in the main text.



Supporting Figure 6. Force-enhanced collagen cleavage by trypsin is observed also in chambers with a different surface treatment. Here, surfaces were blocked with BSA only. Very little force-induced detachment of collagen beads was observed, in contrast to the DDS- and Tween-coated surfaces (Figure 4 and Supporting Figure 5). The trypsin cleavage curve is well described by a double exponential decay; this may arise from the loss of trypsin from solution to the surface and/or contributions from beads tethered to the surface by more than one collagen. Many fewer tethered particles were observed with this surface treatment.

Supporting References

1. Hua, B. et al. An improved surface passivation method for single-molecule studies. *Nat Meth* **11**, 1233-1236 (2014).
2. Shayegan, M. et al. in Proceedings of the SPIE, Vol. 8810. (eds. K. Dholakia & G.C. Spalding) 88101P (SPIE, San Diego; 2013).
3. Yang, D., Ward, A., Halvorsen, K. & Wong, W.P. Multiplexed single-molecule force spectroscopy using a centrifuge. *Nat Commun* **7**, 11026 (2016).
4. Shayegan, M., Altindal, T., Kiefl, E. & Forde, N.R. Intact Telopeptides Enhance Interactions between Collagens. *Biophys J* **111**, 2404-2416 (2016).